Cold Regions Science and Technology, 15 (1988) 289–293
Elsevier Science Publishers B.V., Amsterdam — Printed in The Netherlands

OPTICAL STUDIES OF ANTARCTIC SEA ICE

Elisabeth Schlosser
Institut für Meteorologie und Geophysik, Universität Innsbruck, Innrain 52, 6020 Innsbruck (Austria)

(Received May 9, 1988; accepted in revised form July 12, 1988)

ABSTRACT

During the austral winter 1986 the spectral albedo of both snow-covered and bare sea ice was measured over the wavelength range 400–1350 nm in the eastern Weddell Sea.

The albedo shows high values and a week wavelength dependence in the visible part of the spectrum and a strong decrease with increasing wavelength in the near IR. Maxima in albedo correspond with minima in ice absorption. For relatively thin ice the albedo depends strongly on ice thickness.

Additionally the bidirectional reflectance of sea ice was studied in the laboratory. For ice thicknesses of a few millimeters nearly specular reflectance is found. With growing ice thickness more scattering within the ice occurs and consequently the intensity of the sidewards scattered radiation increases. The reflectance distribution shows a peak in the forward direction which is less developed with thicker ice and smaller crystal size.

INTRODUCTION

The albedo of sea ice strongly influences the energy budget of the ocean–atmosphere system. Whereas the total albedo has often been investigated as a routine part of meteorological work in the Arctic and Antarctic (e.g. Langleben, 1968, 1969, 1971, Hoinkes, 1960, Kuhn et al., 1977), measurements of the spectral albedo of ice and snow surfaces exist only since a relatively short time. Especially lacking are spectral albedo values of young Antarctic sea ice in winter.

Grenfell and Perovich (1981b) determined the spectral albedo of snow in the Cascade Mountains. In the Arctic the spectral albedo of sea ice was studied by Grenfell and Maykut (1977) and Grenfell and Perovich (1984). Kuhn and Siogas measured the spectral albedo of snow and ice in Antarctica and in the Austrian Alps (Kuhn and Siogas, 1978; Kuhn and Stockinger, 1982). The bidirectional reflectance of alpine and polar snow was studied by Kuhn (1985).

With modern remote sensing techniques it is possible to investigate large areas of snow and ice surfaces. However, for the correct interpretation of data obtained by satellite measurements or aerial photography in situ measurements of high spectral resolution are still necessary.

During the austral winter 1986 spectral albedo measurements of sea ice were carried out in the eastern Weddell Sea. Additionally, studies of the bidirectional reflectance of sea ice were carried out in the laboratory.

SPECTRAL ALBEDO

Measurements

The spectral albedo of both snow-covered and bare sea ice was measured over the wavelength range 400 to 1350 nm in steps of 50 nm. Since the intensity of the incoming radiation was very low in the IR wavelengths because of the high latitude and the time of the year, it was not always possible to measure the whole wavelength range. The instrument used was an ISCO spectrometer of 15 nm half width in the visible and 30 nm in the near infrared part of the spectrum. The wavelength could be chosen by

0165-232X/88/$03.50

use of an interference filter. The spectrometer was equipped with a 2π-diffuser disc mounted on a 0.8 m light pipe, so that the receiver could be set up at the end of an aluminium support at a height of about 40 cm above the ground. To avoid uncertainties in wavelength adjustment at a given wavelength the incoming radiation from both the upper and the lower hemisphere was measured. Then the next wavelength was chosen and the process repeated.

Special attention was given to the albedo of thin ice. In recently refrozen leads the ice thickness varied between a few millimeters and about 30 cm. For ice thicknesses larger than 10 cm it was possible to measure directly from the lead surface. When the ice was thinner, the spectrometer was set up close to the edge of the lead.

Results

Most of the measured albedos show a maximum in the visible range (between 500 and 700 nm); a strong wavelength dependence does not occur here. Beyond 700 nm the albedo decreases with increasing wavelength. A secondary maximum occurs at about 1100 nm due to a minimum in ice absorption. In many of the curves a third (little) peak is found at about 850 nm.

Figure 1 shows the absorption coefficient k of ice in dependence on wavelength. Obviously the albedo maxima agree well with the minima in absorption. Even the slight decrease of the absorption coefficient at about 1300 nm can be found in the albedo curves, since the albedo increases at these wavelengths.

Figure 2 shows the spectral albedo of windblown snow (1) and slush (2). Both curves show the typical features described above with a distinct secondary maximum at 1100 nm. Whereas windblown snow has a very high albedo (larger than 90% in the VIS), the values of slush are about 30% lower.

The albedo is mainly determined by volume scattering in the near surface layers of the snow cover or the ice. For spherical grains it decreases with increasing grain size. The possibility that a photon is scattered is given at the air–ice interfaces, whereas it can be absorbed on its way through the ice. With increasing grain size the distance the photon has to travel through the ice between scattering processes

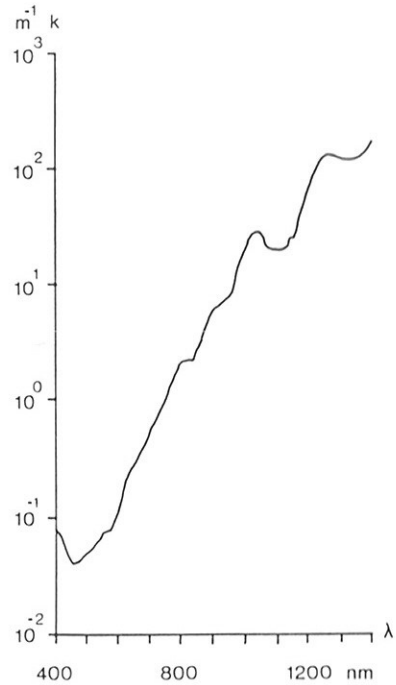

Fig. 1. Spectral absorption coefficient k of ice (after Grenfell and Perovich, 1981a).

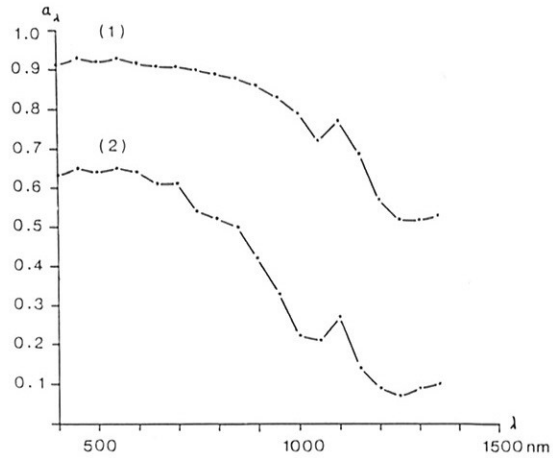

Fig. 2. Spectral albedo of windblown snow (1) and slush (2).

increases too (Warren, 1982). In case of non-spherical grains the volume/surface ratio has to be considered instead of grain size, but the principle described above is still valid. Thus windblown snow, which consists of flat platelets or needles, has a high albedo. Liquid water in the snow cover lowers the

albedo by increasing the effective grain size, since the refraction index of ice and water is nearly the same (Warren, 1982). Therefore slush has a definitely lower albedo than dry snow.

Figure 3 shows the spectral albedo of bare sea ice for different ice thicknesses. It shows a strong dependence on ice thickness. Grease ice of 1.5 cm thickness (curve 1) has a very low albedo (around 16% in the VIS, in the IR the intensity of the radiation was so low compared to the occurring variations that no reasonable measurement was possible.) With growing ice thickness the albedo increases. Nilas of 5 cm thickness (curve 2) has an albedo of about 35% in the VIS, whereas the albedo of thicker ice ($d=11$ cm) (curve 3) reaches values up to 60% or even higher. Curve 2 and 3 distinctly show the decrease of the albedo in the IR, which can also be found in Fig. 2. The secondary maximum at about 1100 nm can only be guessed because of the limited wavelength range.

Considering the fact that sea ice is predominantly snow-covered, the albedo of fresh snow should also be investigated here. Figure 4 shows the spectral albedo of fresh snow. Fresh snow, which has undergone little metamorphosis, has a small volume/surface ratio, so that very high albedo values (larger than 90%) occur in the VIS. Beyond the secondary maximum at 1100 nm the albedo decreases strongly down to values below 50%.

All albedo curves shown here have been measured under totally overcast conditions (10/10 stratus). Therefore errors due to a change in incoming radiation between two measurements (upper and lower hemisphere) or due to a partly specular reflectance of the direct component of solar radiation can be nearly excluded.

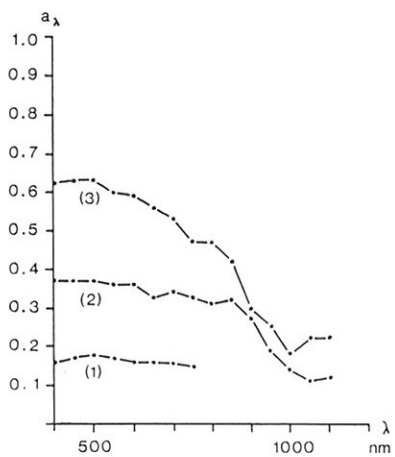

Fig. 3. Spectral albedo of bare sea ice: (1) $d=1.5$ cm (grease ice); (2) $d=5$ cm (dark nilas); (3) $d=11$ cm.

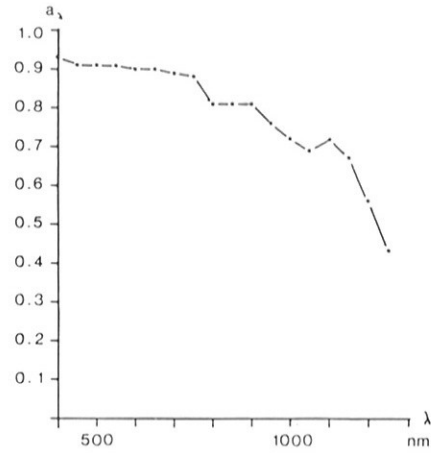

Fig. 4. Spectral albedo of fresh snow.

BIDIRECTIONAL REFLECTANCE

Measurements

Ice was grown by freezing of natural sea water in a tub (63 cm in diameter, 36 cm in height) in a cold room at -4 °C and at -27 °C. A slide projector with a narrow angle beam was used as artificial light source.

The radiance reflected from the ice was measured with a photometer as a function of zenith angle θ_i of the incident ray and zenith and azimuth angle of the reflected ray, θ_r and φ_r, respectively. Figure 5 shows the reflection geometry. The zenith angle of the incident ray was varied between 68° and 61°, θ_r between 61° and 73°. The azimuth angle of the reflected ray φ_r was varied between 0° and 60° in steps of 10°. The measurements were carried out at -4 °C.

Thin sections and salinity profiles of the artificial ice show that it is quite similar to thin ice on recently refrozen leads.

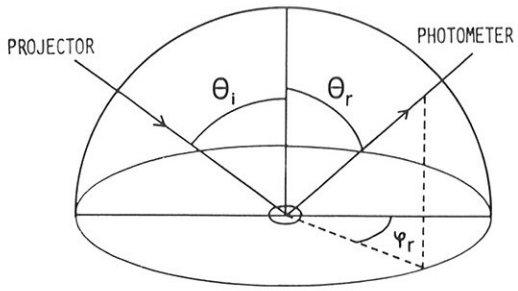

Fig. 5. Reflection geometry.

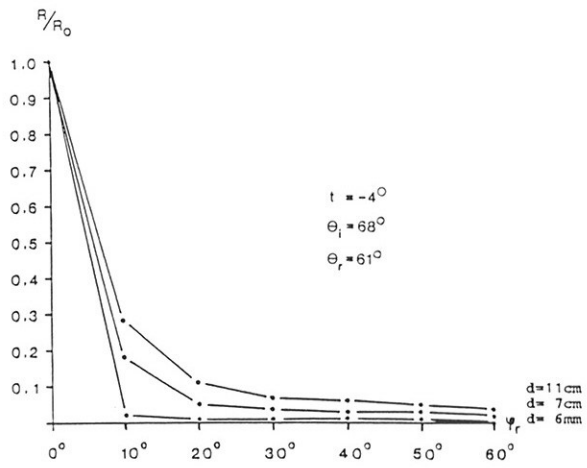

Fig. 6. Reflected radiance vs. azimuth angle φ_r for different ice thicknesses (values are normalized by $R(\theta_r,\varphi_r)/R(\theta_r,0)$, θ_i, θ_r zenith angle of incident and reflected ray, respectively).

Results

Figure 6 shows the reflected radiance versus azimuth angle φ_r for different ice thicknesses. The values are normalized by $R(\theta_r,\varphi_r)/R(\theta_r,0)$. The reflectance distribution shows a peak in the forward direction, which is less developed with thicker ice. For very thin ice ($d=6$ mm) nearly specular reflectance is found. With growing ice thickness more scattering within the ice occurs and consequently the intensity of the sidewards scattered radiation also increases. Scattering in the ice is possible at grain boundaries, brine inclusions and air bubbles. Thus it depends on grain size and grain orientation, salinity, and number of air bubbles.

Whereas the ice in Fig. 6 was frozen at -4°C, Fig. 7 shows the reflectance distribution for ice frozen at -27°C. The peak in the forward direction is less developed with the colder ice. Ice at -27°C and 5 cm thickness has already higher relative intensities of the reflected radiation than -4°C ice of 11 cm thickness. Since the -27°C ice has smaller grain sizes than the -4°C ice due to the higher growth rate, it has more grain boundaries per volume, which could explain the higher scattering. Besides, at -27°C the ice is below the eutectic point, so that scattering is enhanced by salt crystals.

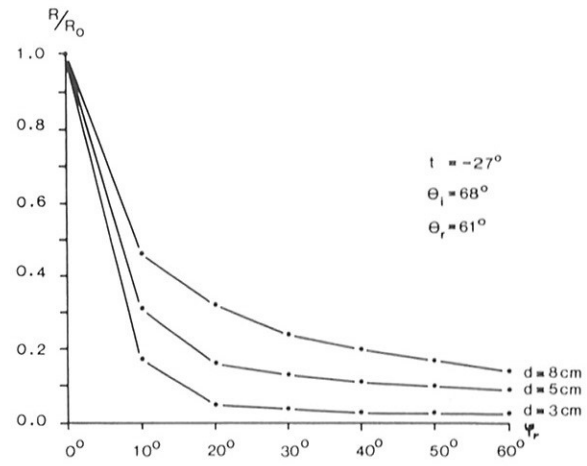

Fig. 7. Reflected radiance vs. azimuth angle φ_r for different ice thicknesses (values are normalized by $R(\theta_r,\varphi_r)/R(\theta_r,0)$, θ_i, θ_r zenith angle of incident and reflected ray, respectively).

A look at the reflectance distribution for different reflection angles θ_r shows that the sidewards decrease in intensity has a maximum when the reflection angle equals or almost equals the incidence angle. Likewise the total intensity reaches maximal values when the incidence angle equals the reflection angle, whereas at higher or lower reflection angles the intensities decrease, again a hint for the large amount of specular reflectance.

No fundamental difference was found between measurements with white and red light; (to produce the red light a Schott filter (RG2) was used.) The spectral variation of the bidirectional reflectance needs further investigation.

CONCLUSIONS

The albedo is mainly determined by volume scattering in the near surface layers of the snow cover

or the ice. Whereas in the VIS, high values and a week wavelength dependence are found, it decreases strongly with increasing wavelength in the near IR. Maxima in albedo correspond well with minima in ice absorption. For relatively thin ice a strong dependence on ice thickness can be observed.

The bidirectional reflectance of sea ice strongly depends on ice thickness and ice structure. The high anisotropy which is found for very thin ice decreases with increasing ice thickness and decreasing grain size due to the enhanced volume scattering within the ice.

It would be very interesting to investigate also the spectral variation of the bidirectional reflection.

ACKNOWLEDGEMENTS

The measurements presented here were performed as part of a Master's thesis at the Institut für Meteorologie und Geophysik, Universität Innsbruck.

I would like to thank Prof. Dr. Michael Kuhn, who gave me the opportunity to participate in the Weddell Sea Project, for his continuous support during my studies.

Special thanks are due to Jose L. Ardai for help in the Antarctic field work.

The project was supported financially by the Geophysical Commission of the Austrian Academy of Sciences and by Deutscher Freundes- und Fördererkreis der Universität Innsbruck e.V.

REFERENCES

Grenfell, T.C. and Maykut, G.A. (1977). The optical properties of ice and snow in the Arctic Basin. J. Glaciol., 18: 445–463.

Grenfell, T.C. and Perovich, D.K. (1981a). Radiation absorption coefficient of polycrystalline ice from 400–1400 nm. J. Geophys. Res., 86(C8): 7447–7450.

Grenfell, T.C. and Perovich, D.K. (1981b). Spectral albedo of an alpine snow pack. Cold Regions Science and Technology, 4(2): 121–127.

Grenfell, T.C. and Perovich, D.K. (1984). Spectral albedos of sea ice and incident solar irradiance in the Southern Beaufort Sea. J. Geophys. Res., 89: 3573–3580.

Hoinkes, H.C. (1960). Studies of solar radiation and albedo in the Antarctic (Little America V and South Pole, 1957/58). Arch. Met. Geophys. Biocl., Ser. B, 10(2. Heft): 175–181.

Kuhn, M., Kundla, L.S. and Stroschein, L.A. (1977). The radiation budget at Plateau Station, 1966–67. Paper 5. In: Meteorological Studies at Plateau Station, Antarctica, Antarctic Res. Ser., 25.

Kuhn, M. and Siogas, L. (1978). Spectroscopic studies at McMurdo, South Pole, and Siple Stations during the austral summer 1977–78. U.S. Antarctic J., 13: 178–179.

Kuhn, M. and Stockinger, F. (1982). Die spektrale Albedo von Schnee und Eis. 17. Internationale Tagung für alpine Meteorologie, Berchtesgaden, 21–25.9.82, Kurzfassung der Vorträge, Selbstverlag des DWD, Offenbach, pp. 282–83.

Kuhn, M. (1985). Bidirectional reflectance of polar and alpine snow surfaces. Ann. Glaciol., 6: 164–167.

Langleben, M.P. (1968). Albedo measurements of an Arctic ice cover from high towers. J. Glaciol., 7: 289–297.

Langleben, M.P. (1969). Albedo and degree of puddling of a melting cover of sea ice. J. Glaciol., 8: 407–412.

Langleben, M.P. (1971). Albedo of melting sea ice in the Southern Beaufort Sea. J. Glaciol., 10: 101–104.

Warren, S.G. (1982). Optical properties of snow. Rev. Geophysics and Space Physics, 20(1): 67–89.